Tellus (1991), *43A*, 97–105

Numerical simulation of the bore-like cold front of 8 October 1987 in Southern Germany

By SABINE P. HAASE, *Meteorologisches Institut, Universität München, Theresienstrasse 37, 8000 München 2, Germany*

(Manuscript received 29 January 1990; in final form 18 September 1990)

ABSTRACT

This paper describes numerical simulations of the bore-like structure of a cold front. The calculations were motivated by a particularly well-documented case study of a dry cold front with this type of structure that occurred on 8 October 1987 in southern Germany. The leading edge of the cold front appeared to have evolved from the amalgamation of cold air outflows from thunderstorms that had earlier developed on the front. These outflows transformed into an undular bore-type disturbance as they moved into a shallow, surface-based stable layer. The numerical simulation reproduces the structural characteristics of the front well.

1. Introduction

On 8 October 1987, a dry cold front crossed southern Bavaria accompanied by a series of spectacular roll clouds. The front was the first of several that were documented in detail as part of the German Front Experiment 1987 (Hoinka et al., 1988). Photographs of the roll clouds (Hoinka and Smith, 1988, Figs. 1, 2) show them to be similar in appearance to morning glory clouds which are observed regularly in northern Australia. Some morning glories are manifestations of an undular bore propagating on a surface-based stable layer. A characteristic of the morning glory environment is the presence of a deep neutrally-stable layer above the stable layer. Morning glory-type disturbances are known to occur elsewhere in the world including other parts of Australia. There are also indications that sometimes morning glory-type disturbances are associated with cold fronts, but relatively few have been documented in detail. A review of morning glories and related types of travelling bore waves in the lower atmosphere is given by Smith (1988).

Brundidge (1965) gave one of the first documentations of a cold front with a large amplitude wave at its leading edge as the front propagated into a prefrontal surface-based stable layer. Many observational and theoretical studies relating to the low-level structure of cold fronts have been carried out since that work appeared and these are reviewed by Smith and Reeder (1988). However, no case of a surface cold front with a wave at its leading edge has been documented in detail. In this respect, the front of 8 October 1987 is unique. For this, numerous data are available from aircraft and the single Doppler radar from the DLR Institute for Atmospheric Physics in Oberpfaffenhofen near Munich. There are surface network data and serial rawinsonde soundings at time intervals of up to 90 min at 6 locations, one situated in Munich, the others along the northern side of the Alpine base line. A complete listing of the data available is given by Hoinka et al. (1990).

The origin of the disturbance observed on 8 October 1987 can be explained to the extent that the cold front can be considered to have had the local structure of a gravity current. There had been heavy shower activity accompanying the cold front a few hours prior to the time of observation of the roll clouds, but this was subsequently left behind. Across southern Bavaria, the front was dry. Hoinka et al. (1990) hypothesize that a shallow gravity current evolved at the low-level leading edge of the front as a consequence of the cold air outflow from the showers. This gravity current then travelled eastwards with all appearances as the continuation of the surface cold front.

The Hoinka et al. (1990) hypothesis is that the observed disturbance was generated when the gravity current moved into a surface-based stable layer with weakly stable stratification above. A simplified version of this configuration in which the stable layer is capped by a deep neutral layer has been studied numerically by Haase and Smith (1989a, b). Basically 3 types of flow were found. The flow in the case of a neutral initial state has the characteristics of a steadily propagating gravity current with a surface-based feeder flow transporting cold air to the elevated head and a return flow in the head itself (Haase and Smith, 1989a). If a strong surface-based stable layer is present before the cold inflow is started, an undular bore is initiated by the intruding air. The bore then propagates on the stable layer ahead of the cold air, an atmospheric example being the morning glory. If the inversion is weak or the inflow Froude number large, the structure of the gravity current itself becomes modified, taking on an undular character with the head circulation partly cut off from the feeder flow. This is an intermediate structure between a gravity current and an undular bore. Disturbances in this regime were called "modified gravity currents" by Haase and Smith (1989b), as shown, e.g., in their Fig. 7. As the depth and stability of the stable layer increase, the head circulation progressively separates, acquiring the structure of a large-amplitude solitary wave with a closed relative circulation. Then the head circulation is followed by further waves increasingly similar to the leading one. Such a succession of waves is of similar structure to a bore itself which is a train of large-amplitude solitary waves, each containing regions of closed circulation. This shows the range of possible disturbance types being generated in such a configuration.

In Section 2 we briefly review the observational data in as much as it relates to the present study. In Section 3, we describe a numerical model simulation of the observed cold front to explore further the Hoinka et al. (1990) hypothesis that it resulted from a gravity current interacting with a surface-based stable layer.

2. The observed front

The observed disturbance passed the DLR in Oberpfaffenhofen at 10:21 GMT accompanied by 3 long straight roll clouds. Isochrones of surface front lines suggest that the disturbance moved with a uniform speed across southern Bavaria. Assuming a two-dimensional disturbance moving with uniform speed, a least-square fit to the times of passage at 14 individual barograph stations gave a translation speed c of 18.1 ms^{-1} in a direction 100° East of North (Hoinka et al., 1990).

The rawinsonde sounding taken in Munich at 09:00 GMT exemplifies the prefrontal conditions over southern Bavaria. Fig. 1a shows the vertical profile of potential temperature derived from this. Prominent is a shallow surface-based stable layer, above which the atmosphere is only weakly stably stratified. Fig. 1b shows the predisturbance profile of the wind component in the propagation direction of the disturbance. At all levels, this wind component u is positive with winds in excess of 14 ms^{-1} between 2600 m and 3600 m.

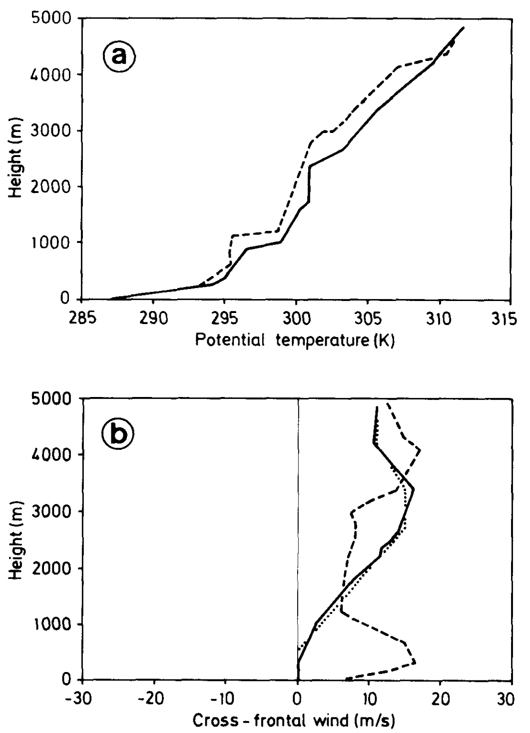

Fig. 1. Vertical profiles of (a) potential temperature and (b) cross-frontal wind component u from the pre- and post-disturbance rawinsonde soundings in Munich at 09:00 (solid) and 12:00 GMT (dashed), respectively. The wind profile as approximated for initialising the model is marked in (b) by the dotted line.

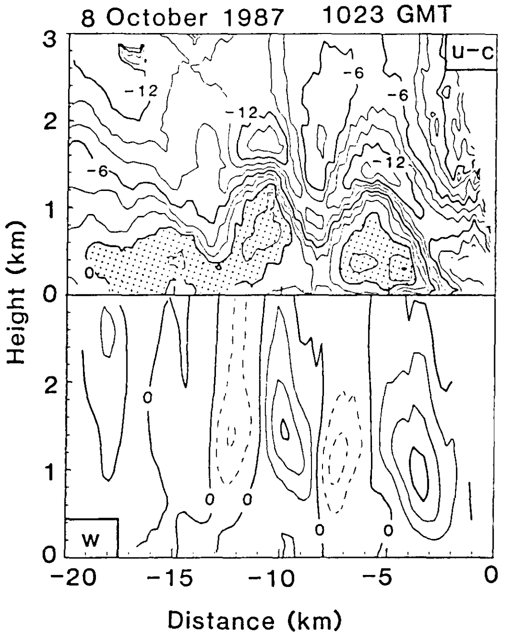

Fig. 2. Vertical cross-sections of the cross-frontal wind component $u-c$ (with disturbance speed $c = 18.1\ \mathrm{ms}^{-1}$) and vertical wind component w as measured by the radar at the DLR at 10:23 GMT on 8 October 1987 (Courtesy of Martin Hagen). Regions of flow faster than the disturbance speed are dotted; contour intervals are $2\ \mathrm{ms}^{-1}$.

Reflectivity patterns as monitored by PPI (plan position indicator) scans of the Doppler radar at the DLR exhibit regions of heavy rain close to Ulm at 9:30 GMT, which is 100 km west of the DLR, somewhat less than 1 h prior to the passage of the roll clouds. Hoinka et al. (1990) surmise that these showers supplied the pool of evaporatively-cooled outflow air that was responsible for the gravity current structure of the cold front at low levels, or possibly for accentuating that already existing*. The scenario is that, as the gravity current moved eastwards, it encountered the surface-based nocturnal inversion that was present in southern Bavaria. The interaction of the gravity current with the prefrontal stable layer would appear to explain the disturbance structure observed in southern Bavaria in the manner described by Haase and Smith (1989b).

* Note that there is some uncertainty as to whether dry cold fronts can develop the local character of a gravity current (Smith and Reeder, 1988).

A vertical cross-section of the cross-frontal wind component u of the disturbance as it approached Oberpfaffenhofen was constructed from the DLR Doppler radar data. Fig. 2 shows a cross-section of u in a frame of reference moving with the disturbance speed c. There is a region of flow faster than the disturbance speed in the leading cell. It is followed by a larger cell and then another weak one. Assuming two-dimensionality, as the long straight roll clouds suggest, each of these 3 regions of maximum u is preceded by regions of strong upward motion, consistent with the occurrence of the 3 roll clouds. There is no continuous feeder flow supplying these cells with colder air, a feature that led to the interpretation of the disturbance as an undular bore. The structural resemblence of the disturbance as shown in Fig. 2 with those of numerically-simulated modified gravity currents shown in Fig. 7 in Haase and Smith (1989b) is striking.

Fig. 19 in Hoinka et al. (1990) shows a composite of the airflow (based on the same data as in Fig. 2) and potential temperature as determined by instrumented aircraft. The surface front line is positioned at 0 km.

3. Numerical simulation of the observed disturbance

The numerical model used here is a two-dimensional nonhydrostatic vorticity-streamfunction model similar to that described in Haase and Smith (1989a). A few modifications were necessary because, in the present case, the stable layer is not capped by a neutral environment in the initial state. Here, a weak stably stratified environment provides at best a leaky wave guide, i.e., one that allows wave energy to radiate away vertically. Hence, the model domain height was increased to 10 km and a damping layer was implemented in the upper third of the domain in the manner described by Crook (1986). To allow for a longer simulation time before the disturbance reaches the right boundary, the domain was extended horizontally to 67.5 km. The grid is stretched vertically with a resolution in the vertical of 34 m near the ground and 150 m at a height of 2 km. The horizontal resolution is 312.5 m as in the original model. The bottom boundary condition includes a surface drag. A further modification is the incorporation of an ambient wind field $u_0(z)$ in the initial state. Now, the steamfunction ψ at the top of the domain ($z=H$) is determined by the initial ambient wind profile $u_0(z)$ with

$$\psi_{z=H}=\int_0^H u_0(z)\,\mathrm{d}z.$$

If a wind profile other than linear with height were chosen, the Coriolis parameter must be set to zero in a two-dimensional numerical model (Reeder and Smith, 1987, page 690). This is justified in the present calculations, since on the time scale of a simulation time of 1 h, Coriolis effects are minor. Note that because we assume $f=0$, the u and v fields are not dynamically coupled in a two-dimensional model and we can neglect the along-front wind component completely.

3.1. Input data

The simulation is initialised with the observed pre-disturbance profiles of potential temperature and the wind field. For potential temperature, the Munich rawinsonde sounding at 09:00 GMT was taken (see Fig. 1a). As this sounding extended only up to a height of 4900 m, the profile was continued by assuming the standard atmosphere lapse rate. The ambient wind profile is approximated from the profile of the across-front wind component u of the same sounding (see dotted line in Fig. 1b). The cold inflow is built up over 240 time steps, which corresponds to 20 min. At the left boundary, below the inflow depth of 2500 m, linear profiles are prescribed for inflow potential temperature deficit and inflow velocity excess. The inflow θ-profile is chosen to have a mean value of $\overline{\Delta\theta}=4$ K, being about the difference between the pre- and post-disturbance soundings in Munich below 2500 m, the latter being at 12:00 GMT. Pre- and post-disturbance soundings in Thalreit and those taken by a motorglider close to the observed roll clouds (see Fig. 18 in Hoinka et al., 1990) show a value for $\overline{\Delta\theta}$ on the order of 6 K. Thus the simulation will be repeated for this value in the sensitivity study in Subsection 3.3. The inflow velocity profile has a mean value of $\overline{\Delta u}=9$ ms^{-1}. This value is estimated from the radar scan at the DLR at 10:18 GMT, which is 3 min before the passage there, compared with that at 11:00 GMT, which is 39 min after the passage (Martin Hagen, personal communication).

A first assessment on the type of disturbance that should result from the input data can be made following Haase and Smith (1989b). They found the quantity $\mu=c_0/c_{gr}$ to characterize the disturbance type, where c_0 is the phase speed for the propagation of infinitesimal amplitude long waves on the stable layer and c_{gr} is the speed of the equivalent gravity current in the absence of the stable layer. Thus, μ is a measure of the strength of the stable layer compared with the inflow strength. For $\mu\leqslant 0.7$, the numerically-simulated disturbances belong to the modified gravity current regime. Following the notation used in Haase and Smith (1989b), we calculate $\mu=c_0/c_{gr}$. Based on the data of the observed disturbance, we obtain the value $\mu=0.3$ as follows. For inflow values of $\overline{\Delta u}=9$ ms^{-1}, $\overline{\Delta\theta}=4$ K, $h_i=2500$ m, $\theta_0=300$ K, we obtain $c_{gr}=c_*(1.01\mathrm{Fr}+0.23)=13.27$ ms^{-1}, where $c_*=[g(\overline{\Delta\theta}/\theta_0)\,h_i]^{1/2}$ and $\mathrm{Fr}=\overline{\Delta u}/c_*$. For a stable layer with $\Gamma=8$ K $(150\text{ m})^{-1}$, $\theta=300$ K and $H=150$ m, we obtain $N=[g\Gamma/\theta]^{1/2}=41.76\times10^{-3}$ s^{-1} and $c_0=2NH/\pi=3.99$ ms^{-1}, whereupon $\mu=0.3$.

This points to a disturbance in the category of a modified gravity current as defined by Haase and Smith (1989b). Note, though, that in these calculations, we have ignored the weakly stable stratification above the low-level stable layer.

3.2. Simulated disturbance

The numerical model was run for the initial state profiles and the inflow parameters as described in Subsection 3.1. Vertical cross-sections of potential temperature θ and relative streamfunction $\psi-\psi_c$ in a frame moving with the leading disturbance are displayed for this simulation at integration times 20, 30 and 50 min in Fig. 3. The panels for θ show the whole computational domain, while those of $\psi-\psi_c$ are for enlarged sections.

The panels for θ and $\psi-\psi_c$ show the evolution of large-amplitude wave disturbances at the leading edge of the cold surge. At $t=20$ min, a single wave has formed and has become partly cut-off from the feeder flow. The forward part of the wave is marked by a strong local maximum in the vertical velocity (not shown). The atmosphere above the surface-based stable layer is weakly stably stratified, thereby allowing waves to propagate vertically. Correspondingly, the isentrope pattern shows the wave axis tilted forwards, indicating that energy is being radiated upwards.

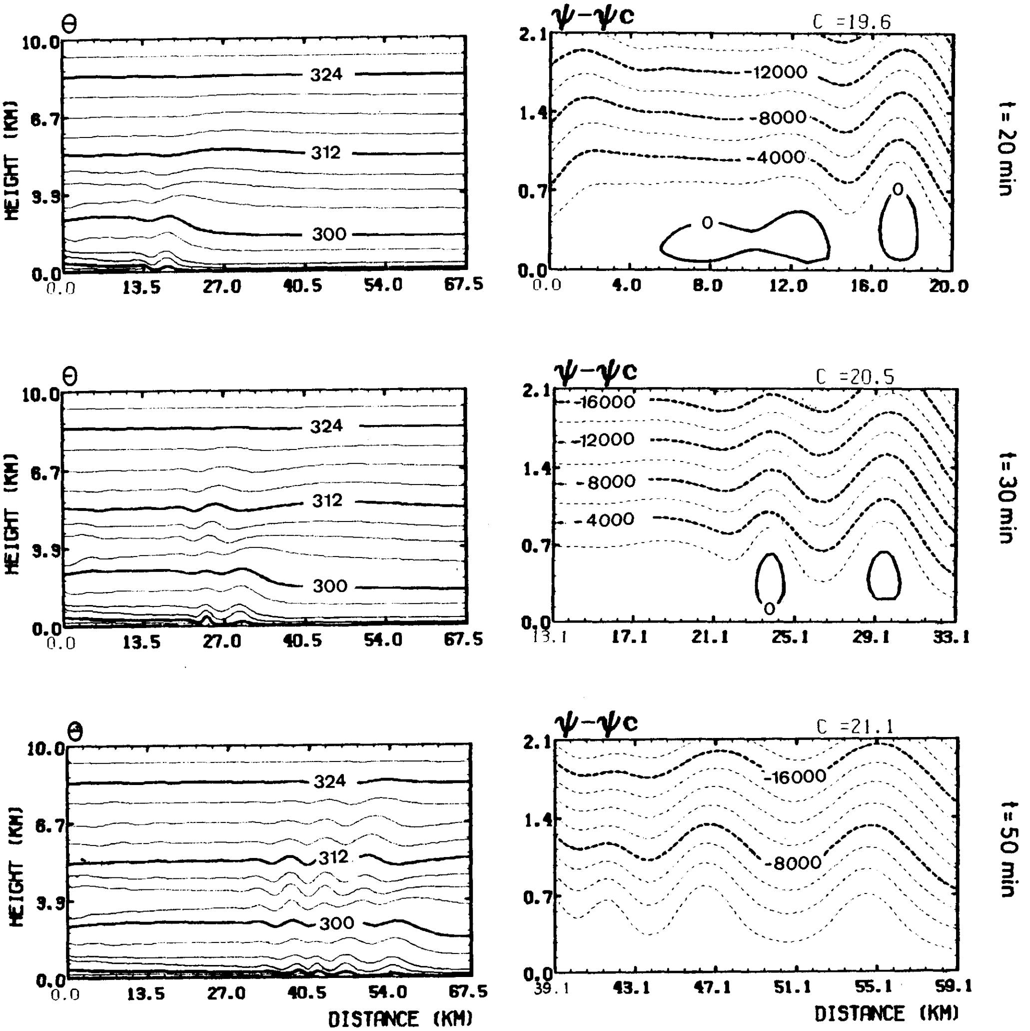

Fig. 3. Time sequence of the numerical simulation based on the observed disturbance with input data as specified in Subsection 3.1. Vertical cross-sections of potential temperature θ (K) and relative streamfunction $\psi - \psi_c$ (m^2s^{-1}) are shown at integration times $t = 20$, 30 and 50 min. Contour intervals are 3 K for θ and 2000 m^2s^{-1} for $\psi - \psi_c$. Note that the panels for $\psi - \psi_c$ show enlarged sections of the computational domain.

As time proceeds, additional waves form, and each in turn becomes cut-off from the feeder flow (see $\psi - \psi_c$ panels); hence the flow field becomes increasingly undular. At times, the waves that have most recently formed ahead of the cold surge have larger amplitudes and are accompanied by a larger w_{max} than were attained by their predecessors (not shown), and accordingly the waves are not ordered in amplitude as predicted by the solution to the initial value problem for the evolution of a long wave of elevation (see, e.g., Christie (1989)). In the latter case, the leading wave has the largest amplitude. This is also mostly, but not always the case for morning glory disturbances in the atmosphere (an exception being the disturbance of 4 October 1979 (Clarke et al., 1981)), and it is the case for the bore-type disturbances as simulated in the laboratory by Wood and Simpson (1984). In

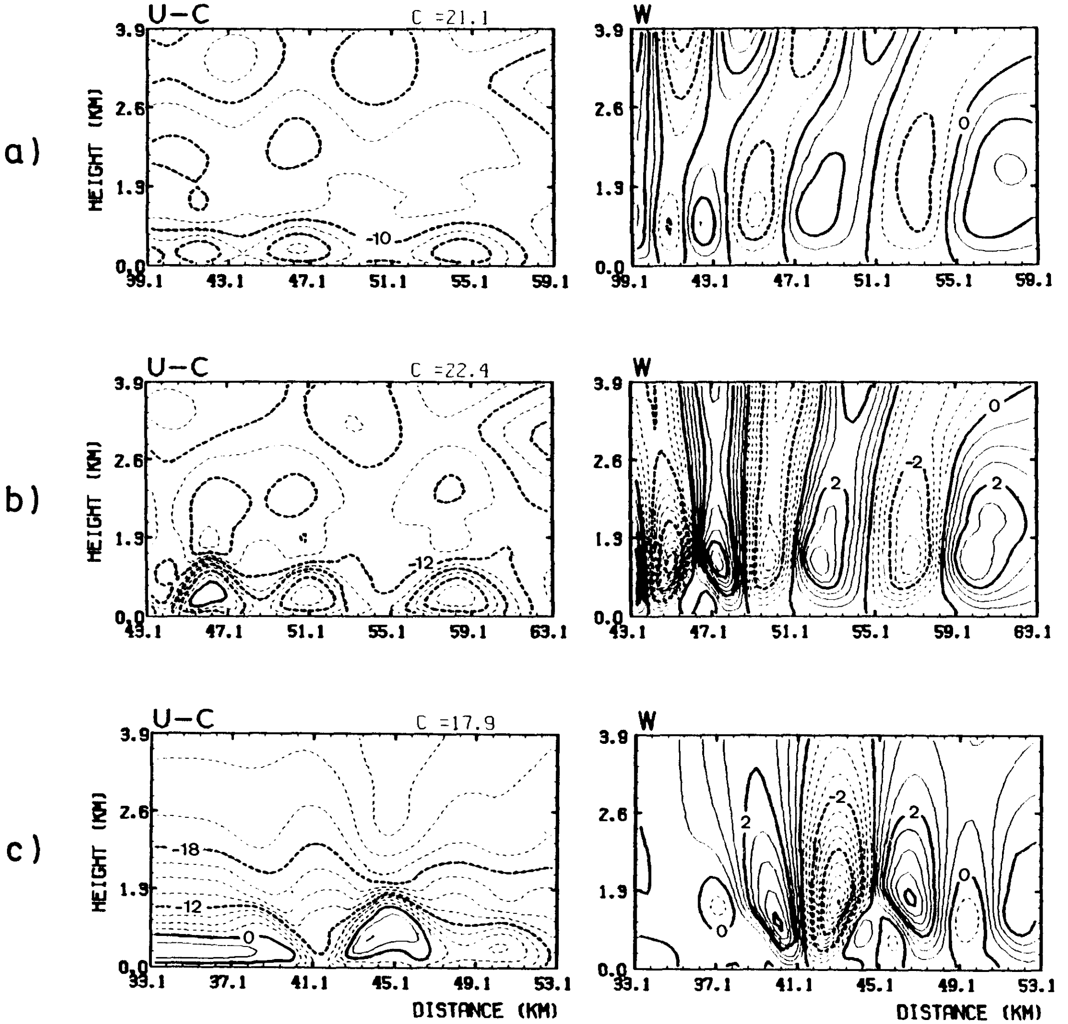

Fig. 4. Cross-sections of relative cross-frontal wind component $u-c$ (ms^{-1}), vertical wind component w (ms^{-1}), potential temperature θ (K) and tracer (labelling the air flowing into the domain) at $t=50$ min for (a) the reference run, as described in Subsection 3.2, (b) the same as in (a) but for mean inflow potential temperature $\overline{\Delta\theta}=6$ K, and (c) the same as in (a) but no ambient wind field. Contour intervals are 2 ms^{-1} for $u-c$, 0.5 ms^{-1} for w and 2 K for θ. Note that while the size of all panels in this figure is the same, their location varies within the computational domain.

the numerical simulation described here, the weakening of the leading waves is presumably attributable to the leaky wave guide.

At $t=50$ min, the 4th wave is strongest, the maximum values of vertical velocity reaching values of -2.6 and 3.1 ms^{-1}. A 5th wave has also started to form. Certainly by the time of this plot ($t=50$ min), the disturbance has not achieved a steady state as in the case of pure gravity currents in a neutral environment. Instead, new vortices form. However, the character of the disturbance as a bore-type phenomenon seems to stay unchanged.

We now attempt to compare the numerically simulated disturbance shown in Fig. 3 with the observed disturbance from 8 October 1987. Of course, such a comparison has intrinsic limitations as it is not possible to determine the exact time at which the comparison should be made. However,

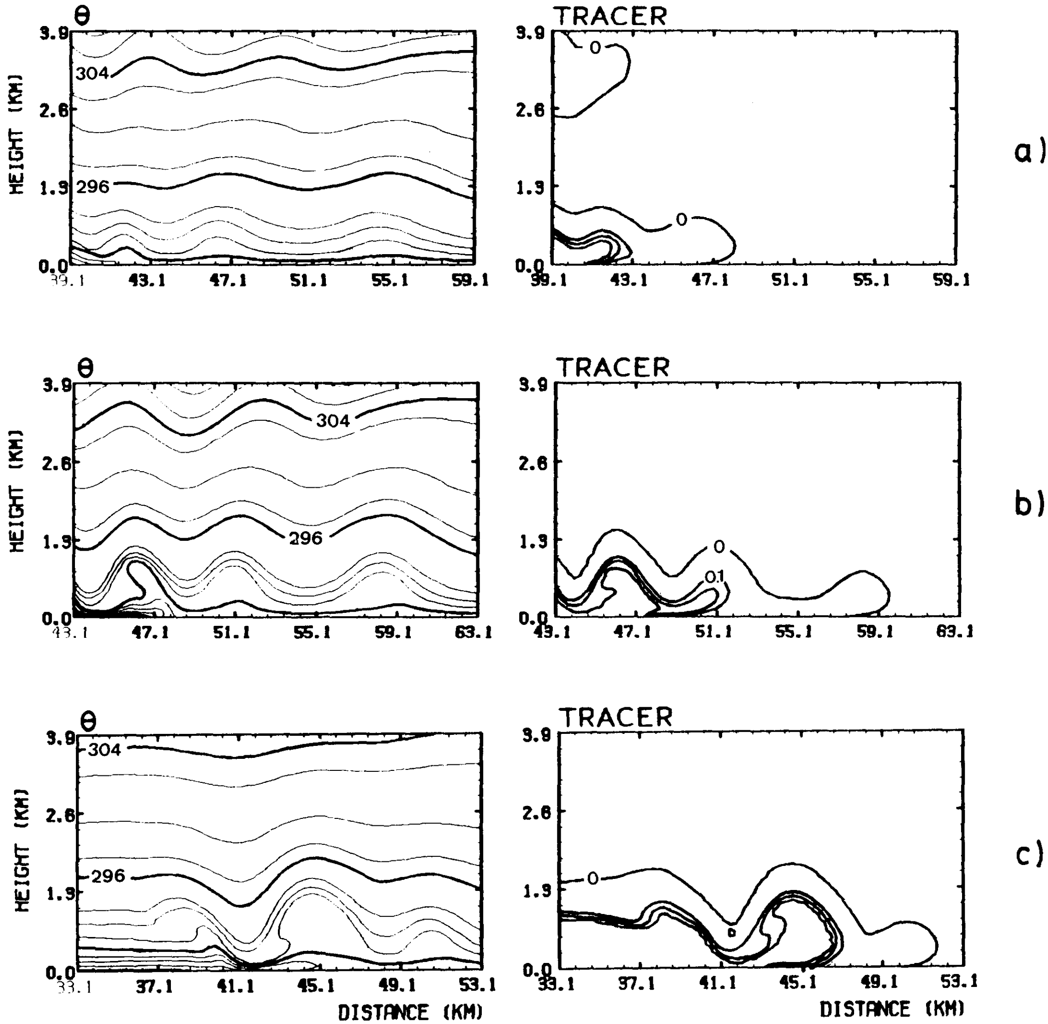

Fig. 4. (continued)

a time of about 1 h would seem appropriate, this being the approximate time between the occurrence of the intense precipitation and the time of observation of the roll clouds at the DLR Institute. This suggests that we should compare the observed disturbance shown in Fig. 2 with the numerical simulation at, say, $t = 50$ min.

Fig. 4 shows vertical cross-sections of the cross-frontal flow $u - c$ in a frame of reference moving with the leading wave, the vertical velocity w, and isopleths of θ and the tracer at $t = 50$ min, on a similar scale as the radar cross-section. There is a striking similarity to the structure of the observed disturbance; in particular, the horizontal and vertical extent of the observed and simulated disturbances are comparable and the vertical motions are of the same order of magnitude. The tracer isolines in Fig. 4a indicate inflow air being carried along by the third wave, even though the $u - c$ panel does not show regions of positive relative flow. This seeming inconsistency is due to the fact that the individual waves propagate at different speeds relative to each other. Fig. 5 shows the horizontal position of the maximum vertical wind

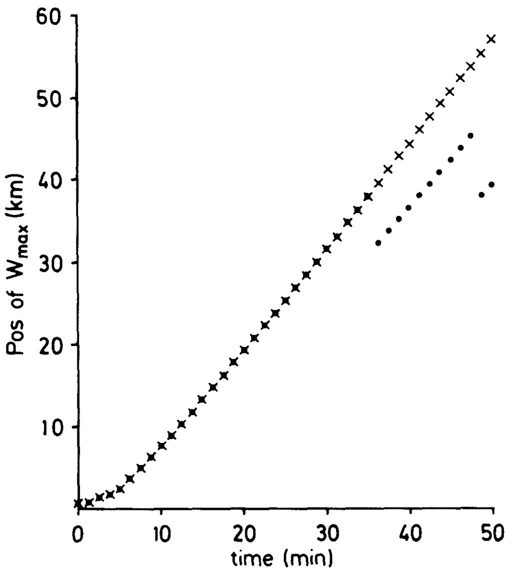

Fig. 5. Time series of the horizontal location (at $z = 1$ km) of the maximum vertical velocity accompanying the leading vortex (crosses) and the respective strongest vortex (dots) for the simulation shown in Fig. 4a.

speed accompanying the leading disturbance (c was determined from this to be 21.1 ms^{-1}) and of the strongest wave as a function of time. The leading wave translates at a constant speed after 10 min. After $t = 40$ min, it decelerates slightly, consistent with the weakening of the leading disturbance due to the loss of energy as observed on Fig. 3. Note that at later times, the leading wave translates faster than the 3rd one, in fact more than 3 ms^{-1} faster; i.e., the 3rd wave has a region of positive relative flow. The radar plot (Fig. 2) also shows positive relative flow in the leading wave. Here, c was determined from the onset times of the observed pressure jumps to be 18.1 ms^{-1}. As the 3 waves are not separately detectable on the barograph traces, this propagation speed might represent a mean value. If here the leading wave propagates faster than the following ones, as was the case for the numerically-simulated disturbance, then the actual propagation speed of the leading wave could be larger than the calculated one. Thus, there would be less positive relative flow in the leading wave than Fig. 2 indicates.

Some difficulties arise when comparing the observed θ-field, mentioned earlier, (see Fig. 19 in Hoinka et al., 1990) with the numerically simulated θ-field in Fig. 4a. For their composite plot, Hoinka et al. (1990) assumed that the main characteristics of the leading edge of the front remained unchanged for about 1 h and that the disturbance was two-dimensional over a very large area. The time-dependent simulation in Fig. 3 suggests that care has to be taken when overlaying the θ-field and the wind fields which were measured about 1 h apart. This is also true for a single aircraft traverse recording potential temperature as this also took almost 1 h to complete. During such a period, the observed waves would have undergone significant evolution, with the leading waves weakening and new waves forming. Thus, such a composite plot cannot be expected to present an accurate picture of the detailed disturbance structure. However, each aircraft traverse (see dotted lines) shows that after the passages of the disturbance, the values for θ stay higher than before as they do in the numerical simulation.

3.3. *Sensitivity study*

The numerical simulation of the disturbance shown in Figs. 3 and 4a was based on data as representative as possible to the observed conditions. While we do not expect to simulate the disturbance in detail, two further simulations will be presented in this section to test the sensitivity of the disturbance structure to the assumptions made about the inflow strength and the initial state.

As pointed out in Subsection 3.1, the data for θ as derived from the radiosonde soundings led to a mean inflow potential temperature $\overline{\Delta\theta}$ of about 6 K, whereas those observed by the motor gliders resulted in $\overline{\Delta\theta} = 4$ K. Thus the same simulation as shown in Fig. 4a was rerun for a $\overline{\Delta\theta} = 6$ K (see Fig. 4b). As expected, a larger $\overline{\Delta\theta}$ results in a larger disturbance that propagates faster and is accompanied by stronger vertical and horizontal motions. At $t = 50$ min, the structure of the 2 simulated disturbances compares well, as judged, for example, by the wavelength of the 3 leading waves. By this stage, the front of the cold air is located a little farther into the third wave than in Fig. 4a. Also, the 4th wave is slightly more pronounced than in the simulation with $\overline{\Delta\theta} = 4$ K (not shown).

On the one hand, there is uncertainty about the accuracy of the observed data. On the other hand, the measured data might not be representative, since the uniformity of the environment in practice is uncertain. An extreme case to assess the impact of one of the assumptions is to compare the simulation that includes an ambient wind field (as shown in Fig. 4a) with the corresponding one without an ambient wind field, see Fig. 4c. Again, waves of similar dimensions have formed and the comparison of Fig. 4a with Fig. 4c is good. We conclude that the broad features of the simulated disturbances are not too sensitive to variations in the ambient wind field, nor to the strength of the inflow.

4. Discussion and conclusions

The foregoing model simulations offer broad support to the hypothesis of Hoinka et al. (1990) that the structure of the cold front of 8 October 1987 over southern Bavaria was produced by the interaction of a gravity current with the surface-based stable layer, showing that this hypothesis provides a dynamically-feasible scenario.

According to Haase and Smith (1989b), the observed and the numerically-simulated disturbances would have been interpreted as modified gravity currents. These have much of the appearance of an undular bore, but differ in detail from a "pure" bore in that cold air which originated in the gravity current is carried along with the large amplitude solitary waves at the leading edge of the bore. In a "pure" bore, there would be no positive relative flow behind the disturbance, and the local cooling that occurs following the bore passage is a result of adiabatic cooling associated with lifting. In modified gravity currents of the type described, local cooling is at some heights *also* associated with the advection of cooler air from the disturbance, air that originated from the initial cold source. Thus the solitary type waves leading the disturbance are not pure solitary waves, in which all the cooling associated with the wave is produced by adiabatic lifting, but are a more complex type containing a region of closed, or approximately closed circulation containing air of source origin.

5. Acknowledgements

I wish to thank Ulrich Schumann, for allowing me to use the DLR-Cray I computer, and Klaus-Peter Hoinka and Martin Hagen for supplying me with the data. I am especially grateful to Roger Smith for many fruitful discussions. Thanks also go to Hilbert Wendt for assisting me with the figures and to Gudrun Fingerle for typing parts of the manuscript.

REFERENCES

Brundidge, K. C. 1965. The wind and temperature structure of nocturnal cold fronts in the first 1.420 Feet. *Mon. Wea. Rev. 93*, 10, 587–603.

Crook, N. A. 1986. The effect of ambient stratification and moisture on the motion of atmospheric undular bores. *J. Atmos. Sci. 43*, 171–181.

Christie, D. R. 1989. Long nonlinear waves in the lower atmosphere. *J. Atmos. Sci. 46*, 1462–1491.

Clarke, R. H., Smith, R. K. and Reid, D. G. 1981. The morning glory of the Gulf of Carpentaria: An atmospheric undular bore. *Mon. Wea. Rev. 109*, 1726–1750.

Haase, S. P. and Smith, R. K. 1989a. The numerical simulation of atmospheric gravity currents. Part I: Neutrally-stable environments. *Geophys. Astrophys. Fluid Dynamics 46*, 1–33.

Haase, S. P. and Smith, R. K. 1989b. The numerical simulation of atmospheric gravity currents. Part II: Environments with stable layers. *Geophys. Astrophys. Fluid Dynamics 46*, 33–51.

Hoinka, K. P. and Smith, R. K. 1988. A dry cold front over southern Bavaria. *Weather 43*, 255–261.

Hoinka, K. P., Volkert, H. and Heimann, D. 1988. *The German front experiment 1987: observations and preliminary results.* DFVLR Forschungsberichte 88–21, 133 pp.

Hoinka, K. P., Hagen, M., Volkert, H. and Heimann, D. 1990. On the influence of the Alps on a cold front. *Tellus, 42A*, 140–164.

Reeder, M. J. and Smith, R. K. 1987. A study of frontal dynamics with application to the Australian summertime "cool change". *J. Atmos. Sci. 44*, 687–705.

Smith, R. K. 1988. Travelling waves and bores in the lower atmosphere: The "Morning Glory" and related phenomena. *Earth-Science Rev. 25*, 267–290.

Smith, R. K. and Reeder, M. J. 1988. On the movement and low-level structure of cold fronts. *Mon. Wea. Rev. 116*, 1927–1944.

Wood, J. R. and Simpson, J. E. 1984. Jumps in layered miscible fluids. *J. Fluid Mech. 104*, 329–342.